Mass Independent Isotopic Fractionation: a key to plasma chemistry

François Robert, Peter Reinhardt

Mass Independent Isotopic Fractionation: a key to plasma chemistry

François Robert[b], Peter Reinhardt[a,1]

[a] *Laboratoire de Chimie Théorique, Sorbonne Université et CNRS, UMR7616, 4 place Jussieu, 75252 Paris CEDEX 05, France*
[b] *Institut Origine et Evolution (O & E), Muséum National d'Histoire Naturelle et Sorbonne Université, IMPMC-UMR 7590 CNRS, 57 rue Cuvier, 75005 Paris, France*

Abstract

We propose a numerical model allowing to calculate the relative variations of isotopic ratios involved in a mass-independent isotopic fractionation (MIF) effect. This model is derived from classical trajectory simulation performed to reproduce the reactions yielding the isotopomers of ozone. In the ozone simulation, we did not introduce quantum mechanical selection rules for trajectories or the potential surface, but we separated instead exchange and non-exchange collisions, in order to introduce the fundamental quantum mechanical requirement according to which, for indistinguishable isotopes, the two possible reaction channels (elastic scattering or particle exchange) have to be superposed. The MIF effect is related to the molecular symmetry of the complex by the result that a different fraction of isotopically asymmetric complexes is stabilized than for symmetric ones.

The model is applied on the results obtained experimentally for Mg and Ti isotopes in plasma. In plasma, Mg and Ti radicals resulting from the molecular dissociation of chlorides react with their parent molecules. In presence of hydrocarbons, isotope exchange rates are greatly enhanced when the intermediate activated complexes are adsorbed at the surface of the carbonaceous grains growing in the plasma. If a chemical reaction with the grain stabilizes the complex faster than its dissociation, MIF effects are observed. In such a chemical situation, the isotopic fractionation greatly exceed the usual theoretical predictions. Several characteristics of the MIF isotopic patterns are reproduced by the model.

Keywords: Mass Independent Isotope Fractionation, Theoretical Model, Plasma Experiments

Highlights

In a plasma, the selection of isotopes by specific chemical reactions does not obey any more the differences of zero point energy between reactants and products.

Introduction

In chemical or isotopic exchange reactions, the partitioning of isotopes always obeys a mass dependent isotopic fractionation law (here referred to as MDF) [1, 2, 3, 4]. For two samples 1 and 2, and two isotopes X and Y, the isotopic fractionation factor α_{x-y} is expressed as:

$$\alpha_{x-y} = \frac{(X/Y)_1}{(X/Y)_2} \tag{1}$$

The sample 2 stands for the initial composition of the reactants and the sample 1 for the products of the reaction studied. Commonly, α_{x-y} is related to the difference in the zero-point energy of the vibrational motion of the different molecular species of the two samples. Taking the example of the three oxygen isotopes, the fractionation factors α_{17-16} and α_{18-16} are found to follow for nearly all terrestrial systems (rocks, liquid water, ice etc) a simple relation,

$$\alpha_{17-16} = \alpha_{18-16}^{\beta} \tag{2}$$

with a exponent $\beta \approx 0.52$. The third decimal of β varies for equilibrium exchange or for kinetic fractionation but β can always be approximated by a function of the difference in isotope masses [3]. Expressing the isotopic fractionation in relative variations (as δ units: $\delta^m\mathrm{O} = (\alpha_{m-16} - 1) \times 1000$), one obtains for oxygen that a variation in $\delta^{18}\mathrm{O}$ is approximately twice that in $\delta^{17}\mathrm{O}$ (see appendix Appendix A).

Contrary to this, solar-system objects (such as the first minerals condensed from the proto-solar gas, the planets and the Sun) exhibit $\delta^{18}\mathrm{O} \approx \delta^{17}\mathrm{O}$ [2, 5, 6]. The discovery of an oxygen isotopic effect in ozone with a similar trend ($\delta^{18}\mathrm{O} \approx \delta^{17}\mathrm{O}$) has opened the question of unusual isotopic fractionation processes [7, 8, 9, 10, 11].

This new isotopic effect observed in ozone is commonly referred to as Mass Independent Fractionation (MIF). Let us notice immediately that this MIF effect in ozone is distinct from other mass-independent effects (not referred here to as MIF) caused by the nuclear magnetic moments of the reactants (MIE i.e. Magnetic Isotope Effect) [12, 13] or by differences in nuclear volumes (NVE i.e. Nuclear Volume Effect) [14].

Since the discovery of MIF in ozone, the details of the effect have been documented by numerous laboratory experiments [15, 16, 17, 18, 19, 20] and its physical origin has been the subject of extensive numerical computations. Classical-trajectory molecular dynamics simulations within an ab-initio

Email address: robert@mnhn.fr (François Robert)

calculated potential surface seem not be sufficient to reproduce the MIF effect in ozone, even when taking into account some purely quantum-mechanical elements (selection of initial rotational states, projection on vibrational states, shift of the potential surface according to ZPEs etc). The observed relation [18] between ΔZPE (the difference in ZPE between the fragments ^{x}O–^{y}O and ^{y}O–^{z}O for a molecule ^{x}O–^{y}O–^{z}O) and the relative rate coefficients has rather confirmed the MDF between the different isotopomers of ozone and was well accounted for by theoretical treatments [22, 23].

Eq. (2) was modified [22] by an empirical fit (the η factor) to reproduce a property of the MIF effect discovered experimentally by Janssen et al. [18]. This empirical fit being valid for almost all the isotopomers of ozone (such as ^{17}O^{16}O^{16}O, ^{18}O^{16}O^{16}O, ^{17}O^{17}O^{16}O, etc.), α_{x-y}, is written in a general form with a mass-dependent term $\alpha^{\mathrm{MD}}_{x-y}$ and a mass-independent term η, identical for all isotope pairs:

$$\alpha_{x-y} = \alpha^{\mathrm{MD}}_{x-y} \times \eta \tag{3}$$

Taking the example of ozone, if the MDF effect is negligible (i.e. $\alpha^{\mathrm{MD}}_{x-y} = 1$), $\alpha^{\mathrm{MD}}_{17-16} = \alpha^{\mathrm{MD}}_{18-16} = 1$ giving $\alpha_{17-16} = \alpha_{18-16} = \eta$ and $\delta^{18}\mathrm{O} = \delta^{17}\mathrm{O}$.

In front of this observation, the origin of η has been searched for numerically around the quantum properties of symmetrical 3-atom complexes (for example ^{18}O^{16}O^{16}O compared to ^{16}O^{16}O^{16}O). Among the most thorough studies on this subject see Refs. [21, 22, 23, 24, 25, 26] who studied the collisional energy transfer and the ro-vibrational energy distribution in reactions forming ozone. Absorption cross section or ozone photolysis were also investigated theoretically [27, 28]. Rao et al. [29] compared the thermal exchange rate constant with that involving indistinguishable isotopes. Yuen et al. [30] studied the role of the vibrational resonances in isotope exchange reactions. Teplukhin et al. [31, 32] computed the scattering resonance lifetimes of the recombination reaction forming ozone and found numerically several MIF effects.

This result [31, 32] gave weight to the interpretation proposed from a classical mechanical approach [33, 34] according to which the lifetimes of the O_3 complexes should be treated differently if these complexes were formed by collisions involving distinguishable or indistinguishable isotopes.

In the present paper, based on the previous simulations on ozone, we show that the relative variations between isotope ratios can be obtained with two free parameters κ and P_I standing for the relative contributions of the reactions involving either dist- or indistinguishable isotopes (that is κ and P_I lying between 0 and 1).

1. Reaction formalism

1.1. Complexes AMB

We consider the following reaction (cf. Fig. 1):
We neglect isotope masses and assume

(i) a 2-isotope system (isotopes A and B) forming possible complexes $X - M - Y$ with M being neither A nor B,

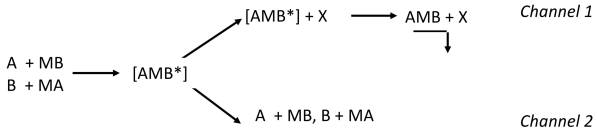

Figure 1: Schematic reaction (with A and B for isotopes and MA and MB for molecular isotopomers) illustrating the fact that only a fraction of the activated complex [AMB*] yields the stable molecule AMB.

(ii) an infinite reservoir of atoms and molecules and

(iii) a continuous reaction flow with two exit channels (complex formation with condensation or re-dissociation).

We obtain (see appendix Appendix B for demonstration) an isotope fractionation of the condensate with respect to the reservoir as:

$$\alpha_{A-B} = \eta = \frac{x_A(1 - \frac{\kappa}{P_I}) + \frac{\kappa}{P_I}}{x_B(1 - \frac{\kappa}{P_I}) + \frac{\kappa}{P_I}} \tag{4}$$

with one parameter, constituted of two components κ and P_I (with values between zero and one) and with the relative abundances of the isotopes A and B noted x_A and x_B ($x_A + x_B = 1$ for a 2 isotope chemical element). Note that, contrary to $\alpha^{\mathrm{MD}}_{x-y}$ the present definition of η depends on the relative abundance (the molar fractions) of the isotopes in the reservoir and is thus not the same for all the chemical elements. This is accounted by the fact that η is the reaction rate ratio and not anymore the rate constant ratio.

Exactly the same relation is obtained for any pair of two isotopes for an element with more than 2 isotopes and complexes $X - M - Y$ (see appendix Appendix B.1).

The mass balance between the Channel 1 and 2 is obtained by replacing in equation 4 the two parameters κ and P_I – analogous to condensation probabilities – by their complement, i.e. $1 - \kappa$ and $1 - P_I$. The fractionation of Channel 2 becomes then:

$$\alpha_{A-B}(\text{channel 2}) = \frac{x_A(\kappa - P_I) + 1 - \kappa}{x_B(\kappa - P_I) + 1 - \kappa} \tag{5}$$

This expression is not any more parametric in κ/P_I, and allows thus to fix the two parameters individually. We will come back to this in the next section.

Equation 4 has the following consequences: if a complex is stabilized by a chemicial reaction faster than its dissociation, MIF effects should be observed. Contrary to the MDF, the magnitude of the isotope effect is not anymore limited by the partition functions of the reactants and η could exceed α_{x-y} by several orders of magnitude (in δ units). This effect, originally predicted in Ref. [9], has likely been observed in plasma where radicals resulting from molecular dissociation react with their parent molecule before being deposited as grains on the walls of the reaction vessel. The chemical reaction with the grain takes place at the surface of the grain where the local high concentration of complexes favors the isotopic exchange.

The magnitude of the MIF effect can be predicted if the two parameters κ and P_I can be calculated. From experimental data

we obtain the inverse path: as we observe a mass-independent fractionation, we can extract the ratio of the two parameters κ and P_I from the data. If Channel 2 can also be analyzed, κ and P_I can be determined individually.

2. Applications

2.1. Ozone

In our previous approach [34], the lifetime of the formation and dissociation reactions $O + O_2 \rightarrow O + O_2$ involving distinguishable isotopes was calculated independently from those involving indistinguishable isotopes. The calculated lifetime ratio (1.183) was then deduced without the need to specify P_I, as this quantity cancelled out in this approach (cf. Appendix Appendix E for the details of the numerical computations).

Considering now a steady-state flow-reactor approach instead of pure gas-phase chemistry, we do not extract η directly from lifetime ratios, but from rate constants or concurrent stabilisation processes with condensation probabilities κ and P_I.

In order to derive for ozone a relation similar to equation 4, two modifications apply: the central atom of the complex is as well of the (multi-isotope) element considered and the abundances of ^{17}O (380 ppm) and ^{18}O (2000 ppm) are negligible relative to ^{16}O (0.9976 $\approx$ 1).

The first modification alters eq. 4 to eq. B.12, see appendix.

Neglecting ^{17}O and ^{18}O, the MIF factor η becomes (eq. C.1)

$$\eta \approx \frac{2}{3}\frac{\kappa}{P_I} + \frac{1}{3} \tag{6}$$

As η becomes identical for ^{17}O and ^{18}O, we see from equation A.2 that the slope in the 3-isotope diagram becomes very close to one.

The 6 isotopomers of $^{16}O^{17}O^{18}O$ result from 6 possible reactions taking place only between distinguishable isotopes. In a scrambled situation, the 6 isotopomers of $^{16}O^{17}O^{18}O$ give on average a calculated α =1.182 when taking into account the MDF (i.e. the ΔZPE). Therefore, for this specific isotopomer, the lifetime ratio is equal to α (see Ref. [34]). This equality between α and the lifetime ratio results from the fact that the combination of the 6 α_{MD} factors for the 6 isotopomers give an overall α_{MD}=1.

The maximum measured isotopic fractionation for $^{16}O^{17}O^{18}O$ was observed for ozone produced by an electric discharge in O_2 (η = 1.203) [35], while photolysis yields somewhat lower η values [36] (down to 1.181). Taking 1.19 as an average value, we obtain in our present formalism an η of $2/3 \times 1.19 + 1/3 = 1.127$. Note that in our previous articles we defined differently, $\eta = \alpha(XYZ)$ (see Appendix Appendix D). Using our values at the point where the lifetime ratio equals 1.183 (i.e. X_R = 0.095, (X_{NR} = 0.905), P_R = 0.720, P_{NR} = 0.237 giving κ=0.283), we can extract P_I with the above determined η of 1.127 as

$$P_I = \frac{2\kappa}{3\eta - 1}$$

and find a numerical value for P_I = 0.238.

This result can be interpreted as follows: 28% and 24% of the complex yielding ozone and formed by collision between dist- and indistinguishable isotopes, respectively, are stabilized as ozone. Note however, that these complexes represent only a minute fraction of the complexes not stabilized as ozone via their encounter with a third body.

If not absolute numbers, one may advance that slightly more complex formed by reactions between distinguishable isotopes (i.e. asymmetrical molecules) are stabilized than those formed between indistinguishable isotopes (i.e symmetrical ones), in a ratio of 7:6.

2.2. Magnesium and Titanium isotopes in chemical plasma mixture of chlorides and hydrocarbons

We have for simple multi-isotope systems $A - M - B$ a slope of

$$S = \frac{\delta_A}{\delta_B} = \frac{x_A - x_C}{x_B - x_C} \tag{7}$$

in a 3-isotope plot with common isotope C (see Appendix Appendix B.1 for demonstration).

This formula is now compared with available data for Mg and Ti isotopes (cf. Appendix Appendix F) whose abundances are not negligible relative to their isotopes ^{24}Mg and ^{48}Ti used to normalize their ratios ($^{25,26}Mg/^{24}Mg$ and $^{46,47,49,50}Ti/^{48}Ti$). We have reported Mg and Ti MIF variations in grains condensed from plasma [37, 38] for two different chemical settings: $MgCl_2$/Pentanol and $TiCl_4$/Pentane for Mg and Ti isotopes, respectively. Data are reported in Figures 2 and 3.

In Figure 2, the calculated slopes S are compared to the data. Both correlations are markedly different from those expected by the MDF theory. The agreement between observed and calculated S is satisfactory. Note that as long as the MDF contribution is negligible, the slope of the correlation does not depend upon the type of chemical reaction involved in the MIF effect. This situation is similar to the MDF theory for which the chemical nature of the isotopically exchanged species has no influence (within ± 0.1‰) on the slope of the MDF correlation.

However, if MDF and MIF variations are commensurable, the slope and the zero-intercept of the linear correlation depend also on the MDF/MIF ratio. This question is not examined here.

We wish to underline that our present approach fulfills the exact mass balance between the two Channels 1 and 2. In other words, the dissociation via the Channel 2 could be calculated by replacing the P values by $1 - P$. In the case of ozone, where the MIF effect was first observed, we only count collision probabilities and the events leading to a stable product of the Channel 1. Channel 2 is inaccessible experimentally, as it is impossible to find in the gas the same molecules of the redissociated complex ($O_3^* \rightarrow O + O_2$). Only ozone molecules and a sample of the whole volume can be analyzed.

The situation is different in experiments where grains are condensed from plasma: spatial isotopic variations were observed in the same grain such as the overall isotopic composition of the bulk grain is restored and does not show the MIF effect (two examples are given in Tables F.2 and F.3). In other terms, the mass balance is satisfied at the scale of the bulk

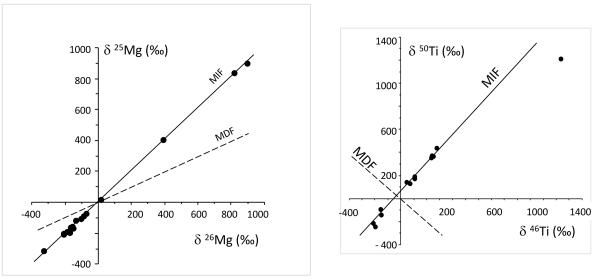

Figure 2: The variations of the magnesium and titanium isotopic compositions of grains condensed in plasma are reported in the 3 isotope diagram: δ^{25}Mg = $f(\delta^{26}$Mg) and δ^{50}Ti = $f(\delta^{46}$Ti) with δ expressed in ‰. In the figure, the present theoretical predictions for MIF without MDF contribution (solid line; δ^{26}Mg = $1.05 \times \delta^{25}$Mg and $\delta^{50}Ti = 1.04 \times \delta^{46}$Ti calculated with, for Mg: x_{24} = 0.7899, x_{25} = 0.100, x_{26} = 0.101 and for Ti: x_{46} = 0.080, x_{48} = 0.738, x_{50} = 0.053) are compared with the MDF variations (dashed line). Data are reported as black dots. The measured variations yield δ^{25}Mg = 1.009 (±0.032) × δ^{26}Mg − 8.3(±4.1) (maximum likelihood; 2-σ error) and δ^{50}Ti = 1.192(±0.086) × δ^{46}Ti + 42.7(±12.9) (maximum likelihood; 2-σ error), in close agreement with the observed correlations. For clarity, error bars are not reported on the figure.

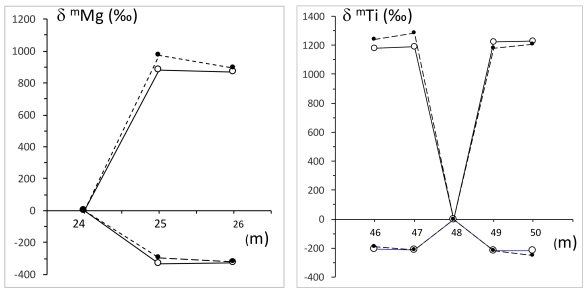

Figure 3: The isotopic patterns are defined as δ^mTi and δ^mMg = $f(m)$ with m being the isotope mass. Positive and negative values stand for the maximum and minimum δ^mMg and δ^mTi values found in the variations measured in the same grain for which the mass balance is satisfied i.e. δ^mMg and δ^mTi ≈ 0 ‰. Data are shown as dashed lines and black dots. The theoretical patterns (solid lines, open symbol) are calculated for Mg with with x_{24} = 0.7899, x_{25} = 0.100, x_{26} = 0.1101, P_I = 0.20 and κ = 0.55 and for Ti with x_{46}= 0.080, x_{47} = 0.073, x_{48} = 0.738, x_{49} = 0.055, x_{50} = 0.053, P_I = 0.08 and κ = 0.33.

grain. These spatial variations span the whole range between minimum and maximum values. For Ti, we have shown that intermediate values can be accounted for by a mixing between two different chemical compounds carrying these minimum and maximum values [39].

We suppose that the minimum and maximum values result from the condensation of two different chemical components produced via the two Channels 1 and 2. If correct, the distribution pattern defined by the 8 independent isotopic compositions $\delta^{46,47,49,50}$Ti(Min) and $\delta^{46,47,49,50}$Ti(Max), reported in Figure 3 should be reproduced with the very same two parameters P_I and κ.

Taking the molar fractions x_m and the observed α_{x-y} or δ_x data, we may extract from eq. 4 values for P_I and κ as free parameters, and we find P_I = 0.08 ± 0.01 and κ = 0.33 ± 0.03. Plugging these again into eq. 4, we can recalculate the isotope fractionation.

The result is shown in Figure 3, where the good agreement between the original data and the reproduction suggests that the mass balance between the two channels is indeed fulfilled.

As expected by the mass balance, if we took all trajectories in the ozone simulations, without the application of a minimum lifetime (i.e. $\tau_{\min}$=0 in equation B.2), we would have obtained $P_R = P_{NR} = P_I = 1$ without any isotope effect. The same is observed for the bulk values in the Mg and Ti experiments.

3. Conclusion

Up to now, numerical efforts to include in models the indistinguishability through different numbering of states, ZPE, resonances and other ingredients of RRKM theory were not sufficient to result in a significant isotope fractionation. In these theoretical considerations the fundamental superposition of like and unlike particles is missing, which leads in our quite crude model naturally to the observed fractionation.

Other reactions documented in the literature can be used to test this model [40, 41]. As mentioned in the Introduction, beside laboratory experiments, numerous mass independent isotopic effects have been observed in meteoritic minerals which are regarded as the first solids condensed during the formation of the solar system. For instance, the solar system variations in oxygen isotopes are interpreted as a self shielding effect [42, 43, 44] i.e. an isotopically selective photodissociation of CO. However, chemical MIF effects similar to those found in ozone are also invoked to interpret these variations [7, 9, 10, 40, 41, 20]. Although this self shielding model remains a viable possibility to produce MIF effects, the present theory represents an alternative interpretation that can be tested in the laboratory by condensation experiments in plasma.

Declaration of interests

The authors declare that they have no known competing financial interests or personal relationships that could have appeared to influence the work reported in this paper.

Author's Contribution

All authors contribute equally to this work.

Acknowledgments

This work has been founded by the ERC Advanced Grant PaleoNanoLife (PI: F. Robert; 161764) and ANR MIF (20-CE49-0011-02). We wish to thank Marc Chaussidon, Mark Thiemens, Dmitri Babikov, Fabien Gatti and Christof Janssen for their time in long debates. We also thank Guillaume Lombardi and Karim Hassouni for their expertise in plasma physics.

Data Availability

Data sharing is not applicable to this article as no new data were created or analyzed in this study.

References

[1] *H.C. Urey*, "The thermodynamic properties of isotopic substances.", J.Am.Chem.Soc. **15** (1947) 562–581

[2] *R.N. Clayton, L. Grossman, T.K. Mayeda*, "A component of primitive nuclear composition in carbonaceous meteorites.", Science **182** (1973) 485–488

[3] *E.D. Young, A. Galy, H. Nagahara*, "Kinetic and equilibrium mass-dependent isotope fractionation laws in nature and their geochemical and cosmochemical significance.", Geochim.Cosmochim.Acta **66** (2002) 1095–1104

[4] *M.F. Miller*, "Isotopic fractionation and the quantification of ^{17}O anomalies in the oxygen three-isotope system: an appraisal and geochemical significance.", Geochim.Cosmochim.Acta **66** (2002) 1881–1889

[5] *M. Chaussidon, G. Libourel, A.N. Krot*, " Oxygen isotopic constraints on the origin of magnesian chondrules and on the gaseous reservoirs in the early Solar System.", Geochim. Cosmochim. Acta. **72** (2008) 1924–1938

[6] *K. McKeegan, A.P.A. Kallio, V.S. Heber, G. Jarzebinski, P.H. Mao, C.D. Coath, T. Kunihiro, R.C. Wiens, J.E. Nordholt, R.W. Moses Jr., D. B. Riesenfeld, A.J.G. Jurewicz, D.S. Burnett*, "The Oxygen Isotopic Composition of the Sun Inferred from Captured Solar Wind.", Science **332** (2011) 1528–1532

[7] *M.H. Thiemens, J.E. Heidenreich III*, "The Mass-Independent Fractionation of Oxygen: A Novel Isotope Effect and its Possible Cosmochemical Implications.", Science **219** (1983) 1073–1075

[8] *J.E. Heidenreich III, M.H. Thiemens*, "A non-mass-dependent oxygen isotope effect in the production of ozone from molecular oxygen – the role of molecular symmetry in isotope chemistry.", J.Chem.Phys **84** (1986) 2129–2136

[9] *R.A. Marcus*, " Mass-independent isotope effect in the earliest processed solids in the solar system: A possible chemical mechanism.", J.Chem.Phys **121** (2004) 8201–8241

[10] *S. Chakraborty, P. Yanchulova, M. H. Thiemens*, "Mass-Independent Oxygen Isotopic Partitioning During Gas-Phase SiO_2 Formation.", Science **342** (2013) 463–466

[11] *C.A.M. Brenninkmeijer, C. Janssen, J. Kaiser, T. Röckmann, T.S. Rhee, S.S. Assonov*, "Isotope Effect in the Chemistry of Atmospheric Trace Compounds.", Chem.Rev. **103** (2003) 5125–5161

[12] *A.L. Buchachenko*, "Magnetic Isotope Effect: Nuclear Spin Control of Chemical Reactions.", J.Phys.Chem.A **105** (2001) 996–1011

[13] *A.L. Buchachenko*, "Mass-Independent Isotope Effects.", J.Phys.Chem.B **117** (2013) 2231-2238

[14] *J. Bigeleisen*, "Second-order correction to the Bigeleisen-Mayer equation due to the nuclear field shift.", PNAS **98/99** (1998) 4808–4809

[15] *M.H. Thiemens, T. Jackson*, "Evidence for the mechanism for production of isotopically heavy O_3.", Geophys. Res. Lett. **15** (1988) 639–642

[16] *J. Morton, J. Barnes, B. Schueler, K. Mauersberger*, "Laboratory studies of heavy ozone.", J.Geophys.Res.Atm. **95** (1990) 901–907

[17] *K. Mauersberger, B. Erbacher, D. Krankowsky, J. Guenther, R. Nickel*, "Ozone isotope enrichment: Isotopomer-specific rate coefficients.", Science **283** (1999) 370–372

[18] *C. Janssen, J. Guenther, K. Mauersberger, D. Krankowsky*, "Kinetic origin of the ozone isotope effect: a critical analysis of enrichments and rate coefficients.", Phys.Chem.Chem.Phys. **3** (2001) 4718–4721

[19] *F. Robert, L. Baraut-Guineta, P. Baraut-Guineta, P. Reinhardt*, "An experimental test for the mass independent isotopic fractionation mechanism proposed for ozone.", Chem.Phys. **523** (2019) 191–197

[20] *M.H. Thiemens, M. Lin*, "Discoveries of Mass Independent Isotope Effects in the Solar System: Past, Present and Future.", Reviews in Mineralogy & Geochemistry **86** (2021) 35–95

[21] *Y.Q. Gao, R.A. Marcus*, "Strange and Unconventional Isotope Effects in Ozone Formation.", Science **293-5528** (2001) 259–263

[22] *Y.Q. Gao, R.A. Marcus*, "On the theory of the strange and unconventional isotopic effects in ozone formation.", J.Chem.Phys. **116** (2002) 137–154

[23] *R. Schinke, P. Fleurat-Lessard*, "The effect of zero-point energy differences on the isotope dependence of the formation of ozone: a classical trajectory study.", J.Chem.Phys. **122** (2005) 094317

[24] *D. Babikov, R.B. Walker, R.T. Pack*, "A quantum symmetry preserving semiclassical method.", J.Chem.Phys. **117** (2002) 8613–8622

[25] *M.V. Ivanov, D. Babikov*, "Collisional stabilization of van der Waals states of ozone.", J.Chem.Phys. **134** (2011) 174308

[26] *M.V. Ivanov, D. Babikov*, "On molecular origin of mass-independent fractionation of oxygen isotopes in the ozone forming recombination reaction.", Proc.Nat.Acad.Sci. **110** (2013) 17708–17713

[27] *S. Ndengué, S. Madronich, F. Gatti, H-D. Meyer, O. Motapon, R. Jost*, "Ozone photolysis: Strong isotopologue/isotopomer selectivity in the stratosphere.", J.Geophys.Res. Atmos. **119** (2014) 4286–4302

[28] *S. Ndengué, R. Schinke, F. Gatti, H-D. Meyer, R. Jost*, "Ozone Photodissociation: Isotopic and Electronic Branching Ratios for Symmetric and Asymmetric Isotopologues.", J.Phys.Chem.A **116** (2012) 12271–12270

[29] *T.R. Rao, G. Guillon, S. Mahapatra, P. Honvault*, "Huge Quantum Symmetry Effect in the O + O_2 Exchange Reaction.", J.Phys.Chem.Lett. **6** (2015) 633–636

[30] *C.H. Yuen, D. Lapierre, F. Gatti, V. Kokoouline, V. Tyuterev*, "The Role of Ozone Vibrational Resonances in the Isotope Exchange Reaction ^{16}O^{16}O + ^{18}O..^{18}O^{16}O + ^{16}O: The Time-Dependent Picture.", J.Phys.Chem.A. **123** (2019) 7733

[31] *A. Teplukhin, D. Babikov*, "Properties of Feshbach and shape-resonances in ozone and their role in recombination reactions and anomalous isotope effects.", Faraday Discuss. **212** (2018) 259

[32] *A. Teplukhin, I. Gayday, D. Babikov*, "Several levels of theory for description of isotope effects in ozone: Effect of resonance lifetimes and channel couplings.", J.Chem.Phys. **149** (2018) 164302

[33] *P. Reinhardt, F. Robert*, "Mass-independent isotope fractionation in ozone", Earth and Planet.Sci.Lett. **368** (2013) 195–203

[34] *P. Reinhardt, F. Robert*, "On the mass Independent isotopic fractionation in ozone.", Chem.Phys. **513** (2018) 287–294

[35] *J. Morton, B. Schueler, K. Mauersberger*, "Oxygen fractionation of ozone isotopes $^{48}O_3$ through $^{54}O_3$.", J. Chem.Phys.Lett. **154** (1989) 143-145

[36] *K. Mauersberger, J. Morton, B. Schueler, J. Stehr*, "Oxygen fractionation of ozone isotopes $^{48}O_3$ through $^{54}O_3$.", Geophys.Research.Lett. **20** (1993) 1031-1034

[37] *F. Robert, M. Chaussidon, A. Gonzalez-Cano, S. Mostefaoui*, "Oxygen and Magnesium Mass Independent Fractionation Induced by Chemical Reactions in Plasma.", PNAS **–** (–) –

[38] *F. Robert, R. Tartese, G. Lombardi, P. Reinhardt, M. Roskosz, B. Doisneau, Z. Deng, M. Chaussidon*, "Mass-independent fractionation of titanium isotopes and its cosmochemical implications", Nature Astronomy **4** (2020) 762–768

[39] *F. Robert, P. Reinhardt, R. Tartese*, "Mass-independent fractionation of titanium isotopes", Chem.Phys **540** (2021) 110970

[40] *S. Chakraborty,M. Ahmed, T. Jackson, M.H. Thiemens*, "Experimental Test of Self-Shielding in Vacuum Ultraviolet Photodissociation of CO.", Science **321** (2008) 1328

[41] *S. Chakraborty,B.H. Muskatel, T. Jackson, M. Ahmed, R.D. Levine, M.H. Thiemens*, "Massive isotopic effect in vacuum UV photodissociation of N_2 and implications for meteorite data.", PNAS **111** (2014) 14704–14709

[42] *H. Yurimoto, K. Kuramoto*, "Molecular Cloud Origin for the Oxygen Isotope Heterogeneity in the Solar System.", Science **305** (2004) 1763–1766

[43] *J.R. Lyons, E. Young*, "CO self-shielding as the origin of oxygen isotope anomalies in the early solar nebula.", Nature **435** (2005) 317–320

[44] *J.R. Lyons*, "An analytical formulation of isotope fractionation due to self-shielding.", Science **282** (2020) 177–200

Appendix A. α and δ notations

In eq. 1 we defined an observable fractionation comparing two samples, and one traces $\delta = (\alpha - 1) \times 1000$ in a three-isotope plot. If a purely mass-dependent fractionation were present, i.e. $\alpha_{ij} = \alpha_{ik}^{\beta}$, we may write $\alpha_{ij} = (1 + \delta_{ij}) = (1 + \delta_{ik})^{\beta} \approx 1 + \beta\,\delta_{ik}$, which leads to a linear relation with slope β. We underline the triviality that if samples 1 and 2 are identical, the fractionation is exactly one, or zero in δ units.

The introduction of the η factor needs two types of samples

– sample 2 standing for the initial composition of the reactants and sample 1 for the products of the reaction studied. In this way we can still write

$$\begin{aligned} \alpha^{1;2}_{18-16} &= \frac{1}{\alpha^{2;1}_{18-16}} = \frac{1}{\alpha^{1;2}_{16-18}} = \alpha^{2;1}_{16-18} \\ \alpha^{1;1}_{18-16} &= \alpha^{1;2}_{16-16} = 1 \end{aligned} \tag{A.1}$$

From eqs. 2 and 3 we may write for 3 isotopes with $\alpha^{\mathrm{MD}}_{A-C} = 1+\epsilon$ and $\alpha^{\mathrm{MD}}_{B-C} = \left(\alpha^{\mathrm{MD}}_{A-C}\right)^{\beta}$:

$$\begin{aligned} \frac{\delta_A}{\delta_B} &= \frac{\alpha^{\mathrm{MD}}_{A-C}\,\eta - 1}{\alpha^{\mathrm{MD}}_{B-C}\,\eta - 1} \\ &= \frac{\alpha^{\mathrm{MD}}_{A-C}\,\eta - 1}{(\alpha^{\mathrm{MD}}_{A-C})^{\beta}\,\eta - 1} \\ &\approx \frac{(\eta-1)+\epsilon\,\eta}{(\eta-1)+\beta\,\epsilon\,\eta} \\ &\approx \left(1+\frac{\epsilon\,\eta}{\eta-1}\right)\left(1-\frac{\beta\epsilon\eta}{\eta-1}\right) \\ &= 1+\frac{(1-\beta)\,\epsilon\,\eta}{\eta-1} - \beta\left(\frac{\epsilon\,\eta}{\eta-1}\right)^2 \end{aligned} \tag{A.2}$$

which allows to estimate the deviation from one in the 3-isotope plot.

With an η of 1.2, and $\epsilon = 0.010$ (i.e. 10‰) we have a approximate slope of $\delta^{18}\mathrm{O}/\delta^{18}\mathrm{O}\ approx 1 + 0.029 - 0.002 = 1.027$.

Appendix B. The equation of the MIF effect

We start from the ozone formation reaction which is considered as a three-body reaction with two exit channels, illustrated in Figure 1. The reaction is simplified in the sense that we consider 2 isotopes, A and B, and a third body M being neither A nor B.

$[AMB^*]$ designates the activated complex resulting from the atom-molecule collisions A–MB (or B–MA). In the following, we do not consider the difference in mass between A and B. In other terms we neglect the mass-dependent isotopic fractionation (that is $\alpha^{MD} = 1$).

We also neglect the possible quantum-mechanical effects like rotational or vibrational selection rules,[21, 22] linked to the symmetry of the complexes [AMA*] or [BMB*].

For introducing the quantum-mechanical principle of indistinguishability, we add a supplementary ingredient: we extract the statistical fraction of exchange (R) and non-exchange (NR) collisions (R and NR are also referred to as Reactive and Non-Reactive) as X_R and $X_{\mathrm{NR}} = 1 - X_R$. X_R is calculated from the respective distribution functions of the lifetimes of the complex, $f_{\mathrm{R}}(\tau)$ and $f_{\mathrm{NR}}(\tau)$, integrated numerically over all τ:

$$X_R = \frac{\int_0^\infty f_R(\tau)\,d\tau}{\int_0^\infty [f_R(\tau) + f_{\mathrm{NR}}(\tau)]\,d\tau} \tag{B.1}$$

We then select trajectories with a lifetime longer than a defined minimal value $\tau_{\min}$ and ascribe the corresponding fraction P of these trajectories to events that possibly form the stable AMB i.e. to Channel 1 (see Figure 1):

$$\begin{aligned} P_{\mathrm{R}}(\tau_{\min}) &= \frac{\int_{\tau_{\min}}^\infty f_{\mathrm{R}}(\tau)\,d\tau}{\int_0^\infty f_{\mathrm{R}}(\tau)\,d\tau} \\ P_{\mathrm{NR}}(\tau_{\min}) &= \frac{\int_{\tau_{\min}}^\infty f_{\mathrm{NR}}(\tau)\,d\tau}{\int_0^\infty f_{\mathrm{NR}}(\tau)\,d\tau} \end{aligned} \tag{B.2}$$

P_{R} and P_{NR} are somewhere between 0 and 1, but do not sum to one. The relative fractions of trajectories for the two kinds of collision events forming three-atom complexes with a measurable lifetime are given by $X_R P_{\mathrm{R}}$ and $X_{\mathrm{NR}} P_{\mathrm{NR}}$. The sum of both terms is necessarily smaller than one.

The product $X_{\mathrm{NR}} P_{\mathrm{NR}}$ corresponds to:

$$X_{\mathrm{NR}} P_{\mathrm{NR}}(\tau_{\min}) = \frac{\int_{\tau_{\min}}^\infty f_{\mathrm{NR}}(\tau)\,d\tau}{\int_0^\infty [f_{\mathrm{NR}}(\tau) + f_{\mathrm{R}}(\tau)\,]d\tau} \tag{B.3}$$

In other words, the term $X_{\mathrm{NR}} P_{\mathrm{NR}}$ stands for the fraction of the non reactive collisions stabilized as AMB relative to the total number of possible collisions forming the complex; and similarly for $X_{\mathrm{R}} P_{\mathrm{R}}$.

As we cannot proceed similarly for collisions involving indistinguishable isotopes (such as A+AM and B+MB forming the stable AMA and BMB products), we use a common value P_{I}, yet unknown. The products AMA and BMB formed via the Channel 1 are in the relative quantity:

$$\underbrace{(X_R + X_{\mathrm{NR}})}_{=1} \times P_I = P_I \tag{B.4}$$

Let us apply these considerations to a flow-reactor with an infinite gas reservoir atoms A and B, and molecules MA, MB, with the isotopic relative abundances noted x_A and x_B, with $x_A + x_B = 1$. We count all the possible collisions A+MA, A+MB, B+MA, B+MB leading to the species AMB, AMA and BMB.

For simplicity, we assume that the intermediate complex has a statistical composition (i.e. is not fractionated relative to the gas reservoir), which means that complexes are distributed as x_A^2 for [AMA*], x_B^2 for [BMB*] and $2x_A x_B$ for [AMB*].

The reactions A+MB and B+MA produce $2x_A x_B[X_{\mathrm{R}} P_{\mathrm{R}} + X_{\mathrm{NR}} P_{\mathrm{NR}}]$ molecules of the type AMB with a lifetime longer than $\tau_{\min}$, which carry as many atoms A as B. For the two molecules AMA and BMB we obtain: $2x_A^2 P_I$ atoms A; and similarly for B.

Depositing these molecules as stable AMA, AMB and BMB, we have then a relative fraction $x'_A = 2x_A^2 P_I + 2x_A x_B(X_{\mathrm{R}} P_{\mathrm{R}} + X_{\mathrm{NR}} P_{\mathrm{NR}})$ of A atoms deposited in AMB and AMA, and $x'_B = 2x_B^2 P_I + 2x_A x_B(X_{\mathrm{R}} P_{\mathrm{R}} + X_{\mathrm{NR}} P_{\mathrm{NR}})$ of B atoms deposited in AMB and BMB.

Introducing $\kappa = X_R P_R + X_{NR} P_{NR}$ and using $x_A = 1 - x_B$, we may simplify

$$2x_A^2 P_I + 2x_A x_B(X_{\mathrm{R}} P_{\mathrm{R}} + X_{\mathrm{NR}} P_{\mathrm{NR}}) = 2x_A\,[x_A(P_I - \kappa) + \kappa] \tag{B.5}$$

The isotopic composition A/B for the Channel 1 is then:

$$\frac{x'_A}{x'_B} = \frac{x_A}{x_B} \times \frac{x_A(P_I - \kappa) + \kappa}{x_B(P_I - \kappa) + \kappa} \tag{B.6}$$

which is always different from x_A/x_B but for the two situations: $x_A = x_B$ and $P_I = \kappa$.

With respect to the reservoir we obtain thus a fractionation

$$\alpha_{A-B} = \frac{x_A(P_I - \kappa) + \kappa}{x_B(P_I - \kappa) + \kappa} \tag{B.7}$$

This fractionation does not depend on masses, but on initial relative concentrations of the different isotopes.

Appendix B.1. MIF beyond complexes AMB

The previous reasoning can be extended to larger multi-isotope systems, for which we distinguish two cases: (i) at least 3 isotopes and (ii) M may be as well one or several atoms of the element under study.

Appendix B.2. More than 2 isotopes

Consider the isotopes A, B, C etc... with $x_A + x_B + x_C + \ldots = 1$, and molecules AMB etc where M is not one of the studied isotopes.

We have:

$$\begin{aligned} x'_A &= 2x_A^2 P_I + 2x_A(\underbrace{x_B + x_C + \ldots}_{1-x_A})(X_{\mathrm{R}}P_{\mathrm{R}} + X_{\mathrm{NR}}P_{\mathrm{NR}}) \\ &= 2x_A\,(x_A(P_I - \kappa) + \kappa) \quad . \end{aligned} \tag{B.8}$$

In δ units this gives

$$\delta_A = (\alpha_{A-B} - 1) \times 1000 = \left(\frac{x_A(P_I - \kappa) + \kappa}{x_B(P_I - \kappa) + \kappa}\right) \times 1000 \tag{B.9}$$

and the slope in the 3-isotope plot becomes

$$\frac{\delta_A}{\delta_C} = \frac{x_A - x_B}{x_C - x_B} \tag{B.10}$$

Appendix B.3. M contains one or more atoms of the element under study

Consider a 2-isotope system, where M contains A and/or B and $n > 0$ in $A - (X)_n - A$ and $A - (X)_n - B$.

molecule	abundance	number of A atoms
$A-(X)_n-B$	$2x_Ax_B$	$1 + n\,x_A$
$A-(X)_n-A$	x_A^2	$2 + n\,x_A$
$B-(X)_n-B$	x_B^2	$n\,x_A$

Table B.1: Distribution of A atoms for a molecule with n inner atoms of the same element.

If we multiply symmetric molecules with P_I, and the asymmetric ones with κ and form the ratio α_{A-B}, we obtain

$$\begin{aligned} \alpha_{A-B} &= \frac{P_I(x_A(2 + n\,x_A) + n\,x_B^2 + 2x_B\kappa(1 + n\,x_A)}{P_I(x_B(2 + n\,x_B) + n\,x_A^2 + 2x_A\kappa(1 + n\,x_B)} \\ &= \frac{(2\kappa + n\,P_I) + 2(n-1)(\kappa - P_I)x_A - 2n(\kappa - P_I)x_A^2}{(2\kappa + n\,P_I) + 2(n-1)(\kappa - P_I)x_B - 2n(\kappa - P_I)x_B^2} \end{aligned}$$

This expression has as limit for $x_A \to 0$

$$\alpha_{A-B} \to \frac{2}{2+n}\frac{\kappa}{P_I} + \frac{n}{2+n}$$

For 2-isotope and 3-atom molecules (i.e. $n = 1$) we obtain

$$\alpha_{A-B} = \frac{(2\kappa + P_I) - 2(\kappa - P_I)x_A^2}{(2\kappa + P_I) - 2(\kappa - P_I)x_B^2} \tag{B.11}$$

with the same limit. Expressed in δ units we arrive at

$$\delta_A = (\alpha_{A-B} - 1) \times 1000 = \left(\frac{(2\kappa + P_I) - 2(\kappa - P_I)x_A^2}{(2\kappa + P_I) - 2(\kappa - P_I)x_B^2} - 1\right) \times 1000$$

Appendix B.4. Both of the previous

For more than 2 isotopes $A-(X)_n-A$, $A-(X)_n-B$, $A-(X)_n-C$ etc. $X_A + x_B + x_C + \ldots = 1$ still holds.

Thus we have to add to table B.1 a line with $B-(X)_n-C$ with abundance $2x_Bx_C$ and $n\,x_A$ atoms of kind A. We arrive for atoms A at $n\,x_A\left[P_I\left(\sum_i x_i^2\right) + \kappa\left(1 - \sum_i x_i^2\right)\right] + 2P_Ix_A^2 + 2\kappa x_A(1 - x_A)$ and thus

$$\alpha_{A-B} = \frac{n\left[P_I\left(\sum_i x_i^2\right) + \kappa\left(1 - \sum_i x_i^2\right)\right] + 2P_Ix_A + 2\kappa(1 - x_A)}{n\left[P_I\left(\sum_i x_i^2\right) + \kappa\left(1 - \sum_i x_i^2\right)\right] + 2P_Ix_B + 2\kappa(1 - x_B)} \tag{B.12}$$

again with the limit $x_B \to 1$ of

$$\alpha_{A-B} \to \frac{n\,P_I + 2\kappa}{n\,P_I + 2P_I} = \frac{2}{2+n}\frac{\kappa}{P_I} + \frac{n}{2+n} \tag{B.13}$$

For a 3-isotope and 3-atom molecule we have:

$$\alpha_{A-B} = \frac{\left[P_I\left(x_A^2 + x_B^2 + x_C^2\right) + \kappa\left(1 - x_A^2 - x_B^2 - x_C^2\right)\right] + 2P_Ix_A + 2\kappa(1 - x_A)}{\left[P_I\left(x_A^2 + x_B^2 + x_C^2\right) + \kappa\left(1 - x_A^2 - x_B^2 - x_C^2\right)\right] + 2P_Ix_B + 2\kappa(1 - x_B)} \tag{B.14}$$

which gives in δ units

$$\delta_A = (\alpha_{A-B} - 1) \times 1000 = \left(\frac{T + 2P_Ix_A + 2\kappa(1 - x_A)}{(T + 2P_Ix_B + 2\kappa(1 - x_B)} - 1\right) \times 1000 \tag{B.15}$$

with $T = \left[P_I\left(x_A^2 + x_B^2 + x_C^2\right) + \kappa\left(1 - x_A^2 - x_B^2 - x_C^2\right)\right]$.

In the 3-isotope plot of oxygen we find again a slope of

$$\frac{\delta_{17}}{\delta_{18}} = \frac{x_{17} - x_{16}}{x_{18} - x_{16}} \tag{B.16}$$

Appendix C. Relation between η and and the lifetime calculated for ozone

Equation 4 is modified to:

$$\alpha_{17-16} = \frac{\left[P_I\left(x_{16}^2 + x_{17}^2 + x_{18}^2\right) + \kappa\left(1 - x_{16}^2 - x_{17}^2 - x_{18}^2\right)\right] + 2P_I x_{17} + 2\kappa(1 - x_{17})}{\left[P_I\left(x_{16}^2 + x_{17}^2 + x_{18}^2\right) + \kappa\left(1 - x_{16}^2 - x_{17}^2 - x_{18}^2\right)\right] + 2P_I x_{16} + 2\kappa(1 - x_{16})} \tag{C.1}$$

This gives for ^{16}O$\approx$ 1:

$$\eta \approx \frac{2}{3}\frac{\kappa}{P_I} + \frac{1}{3} \tag{C.2}$$

Appendix D. Relation between α_{x-y} and $\alpha(XYZ)$

In the literature, two α-notations are used, one for atoms as in eq. 1, and one for molecules as

$$\alpha(XYZ) = \frac{[XYZ]/[16-16-16]_{\text{sample}}}{[XYZ]/[16-16-16]_{\text{standard}}} \tag{D.1}$$

The statistical abundance of ozone molecules XYZ is given as $6x_X x_Y x_Z$, all of distinguishable type, and therefore to be multiplied with κ. Molecules $16-16-16$ are of indistinguishable type, and have to be multiplied with P_I in our model. As the factor of 6 and molar fraction cancel out in eq. D.1 we are left with

$$\alpha(XYZ) = \frac{\kappa}{P_I} \tag{D.2}$$

for the ensemble XYZ, YZX and ZXY. If two atoms are identical, we may have XXY (distinguishable) and XYX (indistinguishable), which yields as sum

$$\alpha(XXY) = \frac{2}{3}\frac{\kappa}{P_I} + \frac{1}{3} \tag{D.3}$$

If all three atoms are identical, we have only situations which are indistinguishable, and, as a consequence,

$$\alpha(XXX) = 1 \tag{D.4}$$

These relations are similar to the limiting cases of α_{X-Y}, but cannot be mapped in a simple way, as in α_{X-Y} all cases of XXX, YYY, XYX, YXY, XXY, YYX and XYZ are regrouped.

Appendix E. Trajectory calculations for ozone

Atom-molecule collisions have been carried out within a classical molecular-dynamics simulation using the potential surface of Bitterova, Schinke et al. Initial conditions (impact parameter, rotational quantum number of the O_2 molecule, initial orientation, kinetic energy of the incoming atom) have been chosen from Boltzmann statistics at fixed temperature.

A delicate point is the determination of a lifetime of a 3-atom complex. One may define a geometrical criterion when to speak of a complex, and when to speak of atom+molecule, and measure the time spent in either situation. This adds technical parameters to the simulations which may be more or less motivated.

We opted for another criterion to distinguish a complex from an elastic scattering situation of an atom and a molecule without any transfer of internal energy. From the kinetic energy of the incoming atom, masses and the scattering angle we can estimate the necessary time-of-flight through a sphere around the target assuming a purely elastic scattering. If the measured time is longer or if an exchange took place, then an intermediate complex had been formed. The lifetime of the complex is the measured flight time minus the time assuming purely elastic scattering.

An ensemble of 3×10^6 trajectories was used for the simulations of one system (temperature, isotope combinations).

Appendix F. Mg and Ti data used to construct the Figures

	δ^{26}Mg	$\pm 2\sigma$	δ^{25}Mg	$\pm 2\sigma$
	-83.3	2.3	-92.5	2.2
	-68.3	6.8	-79.4	7.3
	-99.8	7.9	-112.5	8.4
	-142.9	10.0	-175.3	10.7
	-150.7	10.1	-162.6	10.7
	-167.7	11.2	-198.7	12.0
	-160.5	10.6	-166.5	11.2
	-181.1	12.1	-195.9	12.9
	-184.2	12.2	-194.4	12.9
(*)	21.0	2.0	13.3	2.1
(*)	-131.6	7.0	-122.5	6.7
(*)	-203.6	9.4	-207.0	8.9
(*)	-202.6	12.2	-214.8	11.5
(*)	-321.7	18.8	-320.2	17.8
(*)	398.9	27.1	401.3	25.7
(*)	903.9	39.1	893.5	37.0
(*)	823.6	59.2	828.2	56.2
Bulk	-16.0	1.9	-13.0	1.8

Table F.2: Magnesium isotopic compositions measured in different grains condensed from a plasma composed of $MgCl_2$/Pentanol mixtures[37]. The (*) stands for variations observed in a single grain. The average isotopic composition of (*) is noted as "bulk". Note that 3 outliers of the Mg data have been removed from the published [37] Tables.

	δ^{46}Ti	$\pm 2\sigma$	δ^{47}Ti	$\pm 2\sigma$	δ^{48}Ti	δ^{49}Ti	$\pm 2\sigma$	δ^{50}Ti	$\pm 2\sigma$
	-206.7	36.8	-225.0	38.4	0	-224.1	45.0	-220.8	45.6
	283.5	32.5	393.4	32.3	0	360.5	38.0	431.5	37.6
	-152.7	24.8	-139.6	25.2	0	-94.7	28.8	-98.9	29.3
	254.5	47.3	233.1	49.5	0	306.2	56.1	358.0	55.9
	242.0	24.5	261.6	24.7	0	291.9	28.5	347.2	28.4
	78.0	9.8	94.9	10.3	0	133.2	11.6	124.7	12.0
	52.1	35.0	68.9	36.4	0	94.1	41.9	137.5	41.8
	109.9	33.7	108.5	35.4	0	174.0	40.0	182.2	40.5
(*)	<u>-192.1</u>	95.4	<u>-213.6</u>	140.8	0	<u>-220.6</u>	98.5	<u>-249.9</u>	102.8
(*)	-144.0	28.0	-156.7	49.7	0	-156.2	33.4	-147.0	39.7
(*)	111.2	17.3	133.1	12.3	0	136.0	13.9	167.9	14.9
(*)	244.5	51.9	344.8	31.1	0	324.5	35.6	366.8	50.0
(*)	<u>1241.0</u>	143	<u>1284.4</u>	154	0	<u>1180.5</u>	176	<u>1204.3</u>	180
Bulk	33.2	4.9	61.1	4.7	0	62.9	4.6	92.4	4.6

Table F.3: Titanium isotopic composition measured in different grains condensed from a plasma composed of $TiCl_4$/Pentane mixture.[38] As before (*) stands for variations observed in a single grain. The average isotopic compositions of (*) is noted as "bulk". Underlined values served for determining P_I and κ.